

Multi-wavelength Digital Holographic Microscopy for sub-micron topography of reflecting specimens

Frédéric Montfort^a, Florian Charrière^a, Jonas Kühn^a, Tristan Colomb^c, Etienne Cuche^b, Yves Emery^b, Pierre Marquet^c and Christian Depeursinge^a

^aEcole Polytechnique Fédérale de Lausanne (EPFL), Imaging and Applied Optics Institute, CH-1015 Lausanne, Switzerland, florian.charriere@a3.epfl.ch

^bLyncée Tec SA, PSE-A, CH-1015 Lausanne, Switzerland, www.lynceetec.com

^cCentre de neurosciences psychiatriques, Département de psychiatrie DP-CHUV, Site de Cery, CH-1008 Prilly-Lausanne, Switzerland

ABSTRACT

The study of the internal structures of specimens has a great importance in life and materials sciences. The principle of optical diffraction tomography (ODT) consists in recording the complex wave diffracted by an object, while changing the \mathbf{k} vector of the illuminating wave. This way, the frequency domain of the specimen is scanned, allowing reconstructing the scattering potential of the sample in the spatial domain. This work presents a method for sub-micron tomographic imaging using multiple wavelengths in digital holographic microscopy. This method is based on the recording at different wavelengths equally separated in the \mathbf{k} -domain, of the interference between an off-axis reference wave and an object wave reflected by a microscopic specimen and magnified by a microscope objective. A charged coupled device (CCD) camera records consecutively the holograms, which are then numerically reconstructed following the convolution formulation to obtain each corresponding complex object wavefronts. Their relative phases are adjusted to be equal in a given plane of interest and the resulting complex wavefronts are summed. The result of this operation is a constructive addition of complex waves in the selected plane and a destructive one in the others. Tomography is thus obtained by the attenuation of the amplitude out of the plane of interest. Numerical variation of the plane of interest enables to scan the object in depth. For the presented simulations and experiments, twenty wavelengths are used in the 480-700 nm range. The result is a sectioning of the object in slices of 725 nm thick.

Keywords: digital holography, topography, 3D imaging

1. INTRODUCTION

As the study of the internal structures of specimens has great importance in life and materials sciences, different techniques of optical tomographic imaging have been developed to achieve the reconstruction of the optical properties of 3D specimens. The principle of so-called optical diffraction tomography (ODT) consists in recording the complex wave diffracted by a specimen while changing the \mathbf{k} vector of the illuminating wave. This way, the frequency domain of the specimen is scanned, allowing for the reconstruction of the scattering potential of the specimen in the spatial domain. The theoretical basis of ODT was established in the 1970s by Wolf [1], Carter [2], Dändliker and Weiss [3], and Fercher *et al.* [4] In spite of the great application potential, few successful applications of the ODT techniques to microscopic imaging have been reported, certainly because the accurate recording of the complex diffracted waves may involve complicated implementations. Recently, Charrière *et al.* demonstrated that digital holographic microscopy could successfully be applied to cell tomography [5], obtaining the first quantitative refractive index measurement with an ODT technique applied to a biological specimen. Another way to perform ODT consists of changing the wavelength instead of changing the \mathbf{k} direction. In other words, the frequency domain and specifically the diameter of the Ewald sphere is scanned by changing the wavelength. This technique, developed along the guidelines fixed by the diffraction tomography theorem (see also Refs. 1–4), may appear as rather complex and cumbersome in its practical application. In contrast, digital holography yields a particularly simple way to express indirectly the diffraction tomography theorem: Remaining in the direct space, tomography of the object can be achieved by the superposition of reconstructed wavefronts from holograms taken at multiple wavelengths. This had been proposed several years ago by Marron and Schroeder [6] who called it holographic laser radar. They used an in-line holographic configuration in which the images are focused on the camera. The combination of several phase-shifted acquisitions allows the phase retrieval. Reference to a similar approach

was also described by Arons and Dilworth [7] as Fourier synthesis holography. More recently, the feasibility of section imaging by wavelength scanning digital holography was demonstrated by Kim [8]. In this paper, it is demonstrated that digital holographic microscopy (DHM), allowing us to reconstruct the complex wavefront of an object wave from a single recorded hologram [9-13] is a particularly well-suited technique to achieve multiwavelength tomography. We demonstrate that DHM multiwavelength tomography enables, for the first time to our knowledge, the performance of tomographic imaging with an axial accuracy under the micrometer and a lateral resolution down to the diffraction limit without using a mechanical scan.

2. HOLOGRAM RECONSTRUCTION

The method used to process the simulated holograms is based on a convolution approach. The main advantage of this method is that the pixel sizes of the image and of the hologram are equal. It is therefore convenient to compute the SNR with the formula of Eq. (1) because the correspondence between a reconstructed image point and the initial object point is straightforward. With the other classical Fresnel-Kirchhoff integral reconstruction, described in Refs. 9 and 10, a rescaling of the reconstructed image is necessary for a pixel-to-pixel comparison, which can introduce some additional numerical noise. As described in Ref. 13, the removal of the zero order and of the twin image as well as the spatial filtering are performed by applying a user-defined mask to the Fourier spectrum of the off-axis hologram.

The intensity distribution in the hologram plane can be described by the following expression:

$$I_H(x, y) = \underbrace{O O^*}_{\text{zero order}} + \underbrace{R R^*}_{\text{real image}} + \underbrace{O R^*}_{\text{virtual image}} \quad (1)$$

where O and R are respectively the interfering object and reference. In classical holography, the reconstruction of the wave front is achieved by illuminating the hologram with a replica of the reference wave. The wave front $\Psi(x, y) = R(x, y)I_H(x, y)$ propagates towards an observer, where the three-dimensional image of the object is reconstructed. In digital holography, the reconstruction of the wavefront $\Psi(k\bar{x}, l\bar{y})$, where \bar{x} and \bar{y} are the pixel size of the CCD and k, l are integer values, is obtained the same way by multiplying the hologram intensity distribution $I_H(k, l)$ with a digitally computed reference wave $R_D(k, l)$, called the digital reference wave. Assuming a plane reference wave, R_D can be described as follows:

$$R_D(k, l) = A_R \exp\left[i(k_{D_x} \cdot k\bar{x} + k_{D_y} \cdot l\bar{y})\right] \quad (2)$$

where k_{D_x} , and k_{D_y} are the two components of the wave vector in the hologram plane and A_R is an amplitude constant. The digitally reconstructed wave front $\Psi(k\bar{x}, l\bar{y})$ is first computed in the hologram plane $x_O y_O$, and can afterward be evaluated at any distance from the hologram plane by the calculation of the scalar diffraction of the wavefront in the Fresnel approximation. $\Psi(m\Delta\xi, n\Delta\eta)$ is computed at a distance d from the hologram plane, in an observation plane $O\xi\eta$, by use of the following Fresnel propagation formula:

$$\Psi(m\Delta\xi, n\Delta\eta) = A\Phi(m, n) \times \text{FFT}^{-1} \left\{ \text{FFT} \{ R_D(k, l) I_H(k, l) \}_{p, q} \times \exp\left[-i\pi\lambda d (p^2 + q^2)\right] \right\}_{m, n} \quad (3)$$

where p, q and m, n are integers ($-N/2 \leq m, n < N/2$), FFT is the Fast Fourier Transform operator, FFT^{-1} is the Inverse Fast Fourier Transform operator, $A = \exp(i2\pi d/\lambda)/(i\lambda d)$ is a propagation constant, and $\Phi(m, n) = \exp(-i\pi/(\lambda d_1)m^2\Delta\xi^2 - i\pi/(\lambda d_2)n\Delta\eta^2)$ is the so-called digital phase mask with parameters d_1 and d_2 digitally adjusted to correct the phase aberration due to the microscope objective. $\Delta\xi = \bar{x}$ and $\Delta\eta = \bar{y}$ are the sampling intervals in the observation plane.

Considering only the virtual images of Eq. (1), the propagated wave front corresponding to the computed digital reference wave is:

$$\Psi = R_D R^* O, \text{ with } R_D = \exp\left[i(k_{D_x} \cdot k\bar{x} + k_{D_y} \cdot l\bar{y})\right] \quad (4)$$

where k_{D_x} and k_{D_y} , are two parameters adjusted to achieve identical propagation directions for R and R_D . Eq. 3 requires the adjustment of four parameters for proper reconstruction of the phase distribution. k_{D_x} and k_{D_y} compensate for the tilt aberration resulting from the off axis geometry or resulting from an imperfect orientation of the specimen surface which should be accurately oriented perpendicular to the optical axis. d_1 and d_2 corrects the wave front curvature induced by the microscope objective according to a parabolic model. Note that in the present study, these two last parameters only need to be adjusted during the processing of real acquired holograms, as in the simulation no curvature induced by the microscopy objective was considered. As explained in Ref. 9, the parameter values are adjusted in order to obtain a constant and homogeneous phase distribution on a flat reference surface located in or in the proximity of the specimen. The manual procedure described in Ref. 9 has been implemented here as a semi automated

procedure. First, the program extracts two lines – an horizontal line along 0ξ and a vertical line along 0η – whose location is defined by the operator in the reference surface. Then, one-dimensional (1D) phase data extracted along the two lines are unwrapped in order to remove 2π phase jumps, and a curve fitting procedure is applied to evaluate the unwrapped phase data with a 1D polynomial function of the second order. k_{Dx} and d_1 are iteratively adjusted to minimize the deviation between the fitted curve and the ideal horizontal constant profile. The same way, k_{Dy} and d_2 are adjusted until the vertical profile is as close as possible to the ideal vertical constant profile. In general, less than five iterations are necessary to reach optimal parameters values. If a reference area isn't available on the specimen, the parameters are first calculated on another reference surface (air in transmission, a mirror in reflection), then a simple digital tilt adjustment of the phase, corresponding to an adjustment of k_{Dx} and k_{Dy} , is performed with the same procedure described above when the specimen is observed.

Note that this digital adjustment method has been generalized to a multi-profiles automatic procedure with correction of optical aberrations of higher order. An extensive description of the technique and its applications to specimen shape compensation is presented in Ref. 15.

3. MULTIPLE WAVELENGTHS DHM FOR TOMOGRAPHY

DHM uses a single hologram taken at a single wavelength and with a single propagation direction of the illuminating wave (single k -vector). Thus, the image also contains information coming from the upper and lower sections of the object, which blurs the image and makes this method more suitable for thin objects. Furthermore, the topology of the object is given by the phase information and so it suffers from the phase wrapping problems, which happen when that the object induces a phase shift smaller than the wavelength. It is often not the case and thus an algorithm is needed to unwrap the collected phase. Although these techniques are efficient for relatively smooth objects, their results are in most cases wrong when abrupt edges higher than the wavelength are encountered making the use of DHM with relatively thick objects difficult. The proposed method uses variable wavelengths illumination waves. The reciprocal space is then scanned by changing the diameter of the Ewald sphere. Digital holography yields a particularly simple way to express "indirectly" the diffraction tomography theorem: remaining in the direct space, tomography of the object can be achieved by the superposition of reconstructed wavefronts from holograms taken at multiple wavelengths. Nevertheless, none of the previously mentioned techniques works at the micro-scale [6-8]. The introduction of a microscope objective in the set-up, the use of the retrieved phase for high axial precision measures and a wide wavelength range opens the field of tomography to the sub-microscopic world.

Multiple wavefronts addition principle

To introduce the multi-wavelength approach, let us state that the diffracted fields of a single hologram Ψ_j , reconstructed in the object plane, creates an exact replica of the object wave Ψ_0 at the object. Let us also consider an object point P located at (x_0, y_0, z_0) which emits a Huyghens spherical wavelet proportional to $A(P)\exp(ikr_{PQ})$ measured at an arbitrary point $Q=(x, y, z)$, where $r_{PQ} = n|r_P - r_Q|$ is the optical pathlength between P and Q , and n is the refractive index. We neglect the $1/r$ dependence of the amplitude. The wave propagates along the z -direction. The factor $A(P)$ represents the field amplitude and phase at the object point. For an extended object, the field at Q is proportional to the above wavelet field integrated over all the points of the object:

$$\psi_j(Q) \propto \sum_{j=0}^{N-1} \psi_j(Q) \propto \iiint A(P) \exp(ikr_{PQ}) d^3r_{PQ} \quad (5)$$

The factor $\exp(ikr_{PQ})$ represents the propagation and diffraction of the object wave. Now assuming that a number N of copies of the electric field distribution are generated by varying the wavelength (and thus the wave number k), all the other conditions of object and illumination remaining the same, let's take N k -vectors k_j regularly separated by dk between k_{\min} and k_{\max} . We have: $k_{\min} = 2\pi/\lambda_{\max}$, $k_{\max} = 2\pi/\lambda_{\min}$, $dk = (k_{\max} - k_{\min})/(N-1)$.

The result of the superposition of these electric fields at Q is:

$$\psi(Q) = \sum_{j=0}^{N-1} \psi_j(Q) \propto \iiint A(P) \exp(i\bar{k}r_{PQ}) T(r_{PQ}) d^3r_{PQ} \quad (6)$$

where $\bar{k} = (k_{\min} + k_{\max})/2$.

$T(r_{PQ})$ can be seen as an amplitude filter function with these extremas:

$$T(r_{PQ}) = \frac{\sin\left(dkr_{PQ} \frac{N}{2}\right)}{\sin\left(dkr_{PQ} \frac{1}{2}\right)} \text{ has: } \begin{cases} \text{maximas for } r_{PQ} = n \frac{2\pi}{Ndk}, n = mN \\ \text{minimas for } r_{PQ} = n \frac{2\pi}{Ndk}, n \neq mN \end{cases} \quad (7)$$

If we consider an infinite wavelength range, then $T(r_{PQ})$ becomes a Dirac function and the resulting wavefront $\Psi(Q)$ is non-zero only at P. That is, for a large enough number of wave numbers k , the resultant field is proportional to the field at the object, and non-zero only at object points. In practice, if one uses a finite number N of wavelengths at regular intervals dk then the object image $A(P)$ repeats itself at axial distances $\Lambda = 2\pi/dk$ with axial resolution of $\delta = \Lambda/N$. By using appropriate values of dk and N , Λ can be matched to the axial extent of the object and δ to the desired level of axial resolution.

Practically, several equally k -spaced holograms are experimentally recorded and each hologram is reconstructed independently and stored in its complex form. A reference surface is selected in the field of view. All the wavefronts to be summed are then phase shifted so that the phases in the reference area are set to the same reference value (zero for example). This plane of reference will be the one in which all the unitary vectors will add constructively thanks to the phase adjustment. The points out of this plane will have various phase differences depending on the wavelength, and the unitary vectors will cancel each other when summed. This reference area is to be selected only once. Any further plane of interest distant of an optical path length ε from the plane of reference can be derived without having to select a new reference area: knowing equal phases in the reference area, the phase difference $\Delta\phi$ between the new plane of interest and the reference plane is given by $\Delta\phi = (2\pi/\lambda)/\varepsilon$. Thus each wavefront will be phase-shifted consequently and when added, the complex wavefronts will be constructive in the new plane of interest, allowing scanning the whole sample in depth.

4. RESULTS AND CONCLUSION

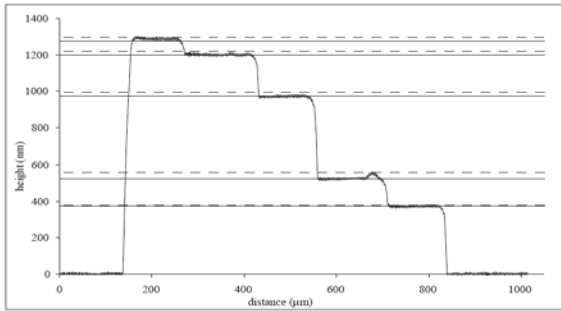


Fig. 1 Ellipsometer measurement of the target used to demonstrate the tomography. It consists of 5 reflecting steps having 375, 525, 975, 1200 and 1275 nm heights. The dashed lines shows the theoretical values, the plain lines the measured values.

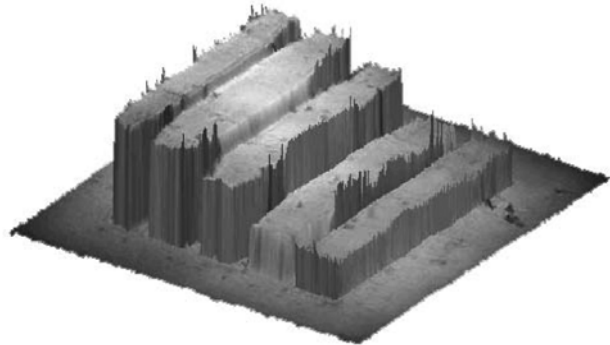


Fig. 2 3D rendering of the reconstructed test target with the DHM topography: for each xy position the height z for which the summation reaches a maximal value is shown.

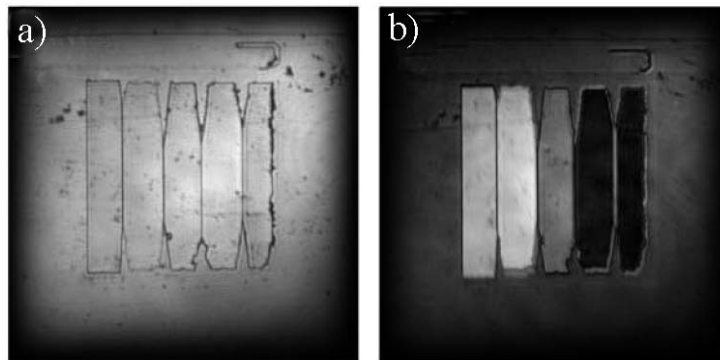


Fig. 3 a) sample amplitudes of the experimental target b) experimental results of a reconstructed sections at a height of 525nm.

Experiments have been done to demonstrate the topographic and 3D imaging abilities. To do so, twenty holograms have been experimentally recorded with regularly k -spaced wavelengths in the 480 - 700 nm range. The absolute value of the amplitude filter created by summing the given twenty wavefronts has the shape given by Eq. 7. The resolution δ is given by the first zeros of the function, and the axial extent Λ by distance between two maximums. With the parameters used in a reflection set-up, the axial resolution is 725 nm and the axial extent 14.5 μm . The target under investigation consists of 5 reflecting steps having 375, 525, 975, 1200 and 1275 nm heights, and was calibrated using an ellipsometer (see. Fig. 1). It is built by structuring silicon oxide (SiO_2) layers on a silicon wafer and recovered with 10 nm chrome and 100 nm gold for a total reflection. The sample is 250 microns large. Nevertheless, due to etching properties, the highest steps are no more rectangular, but have been attacked in the corners. The experimental set-up is based on a classical Mach-Zender off-axis holographic interferometer. The light source is generated by an argon ion plasma laser (Coherent Innova 200) pumping a modelocked Ti:S laser system (Coherent Mira 900). The beam is then amplified by a regenerative amplifier (Coherent RegA 9000) and finally extended in wavelength with a tunable optical parametric amplifier (Coherent OPA 9400). The beam coming from the optical parametric amplifier (OPA) is split. On one side, the object beam illuminates the sample through the microscope objective (MO, focal length 18.4 mm, NA=0.15, magnification of 10 \times) and its diffracted field, collected by the MO, interferes on the CCD with the reference beam. In our case, the interference is done in an off-axis geometry, meaning that a small angle is introduced between both waves. Two more lenses are used: one is the object beam condenser (OC) that focuses the object beam at the back focal length of the microscope objective in order to have a collimated beam illuminating the sample, and the second is the reference lens (RL) that curves the reference beam to match the curvature introduced by the microscope objective on the object beam in the CCD plane. It is to note that the image of the sample through the MO is not focused on the CCD camera.

The results of the tomography is shown in Fig. 2: the reconstructed specimen has been scanned in depth as describe previously in the Chapter 2. The slicing effect of the summation is shown on Fig.3, where the amplitude image of the specimen for a single wavelength (Fig. 3a) is compared to the result of the summation for an height of 525 nm. The 3D rendering (see Fig. 2) shows for each xy position the height z where the summation reaches a maximal value. The imperfections in the reconstruction process, like the adjustment of the reference wave parameters and the filtering of the zero order and twin image, influencing both experimental and simulation results, are negligible. Those like the set-up imperfections (lenses, beam-splitters,...) and the wavelengths precision influence only the experimental data. These last variations affect the amplitude of the filter function, but not its zeros. Thus the attenuation factors can be affected, but not the slicing resolution. We have shown that topography could be achieved at the microscopic scale using Digital Holographic Microscopy (DHM). Simulations and experiments allowed the statement of the method. Slices with a thickness of 725 nm could be achieved, corresponding to the theoretical predictions. This resolution can be improved by taking more holograms in a larger wavelength range. Those results have been achieved using a reflective target to set up the method and the resolution of this new technique. This technique seems promising for 3D bulk specimen investigation.

ACKNOWLEDGEMENTS

This research has been supported by the Swiss National Science Foundation (SNSF) grant 205320-103885/1. Frédéric Montfort's email is frederic.montfort@a3.epfl.ch.

REFERENCES

1. E. Wolf, "Three-dimensional structure determination of semi-transparent object from holographic data, " *Opt. Comm.*, 1, 153–156 (1969).
2. W.H. Carter, "Computational reconstruction of scattering objects from holograms", *J. Opt. Soc. Am.* 60, (3), pp. 306-314 (1970)
3. R. Dändliker, K. Weiss, "Reconstruction of three-dimensional refractive index from scattered waves, " *Opt. Comm.*, 1, 323–328 (1970).
4. A.F. Fercher, H. Bartelt, E. Becker, H. Wiltschko, "Image formation by inversion of scattered field data: Experiments and computational simulation", *Appl. Opt.* 18 (14), pp. 2427-2439 (1979).
5. F. Charrière, A. Marian, F. Montfort, J. Kuehn, T. Colomb, E. Cuche, P. Marquet and C. Depeursinge, "Cell refractive index tomography by digital holographic microscopy," *Opt. Lett.* **31** (2), 178–180 (2006).
6. J.C. Marron, K.S. Schroeder, "Holographic laser radar", *Opt. Lett.* 18 (5), pp. 385-387 (1993).

7. E. Arons, D. Dilworth, "Analysis of Fourier synthesis holography for imaging through scattering materials", *Appl. Opt.* **34** (11), pp. 1841-1847 (1995).
8. M.K. Kim, "Tomographic three-dimensional imaging of a biological specimen using wavelength-scanning digital interference holography", *Opt. Express* **7** (9), pp. 305-310 (1999).
9. E. CuChe, P. Marquet and C. Depeursinge, "Simultaneous amplitude and quantitative phase-contrast microscopy by numerical reconstruction of Fresnel off-axis holograms," *Appl. Opt.*, **38**, 6994-7001 (1999).
10. P. Marquet, B. Rappaz, P. J. Magistretti, E. CuChe, Y. Emery, T. Colomb and C. Depeursinge, "Digital holographic microscopy: a noninvasive contrast imaging technique allowing quantitative visualization of living cells with subwavelength axial accuracy", *Opt. Lett.*, **30**, 468-470 (2005).
11. E. CuChe, F. Bevilacqua, and C. Depeursinge, "Digital holography for quantitative phase contrast imaging", *Opt. Lett.* **24** (5), pp. 291-293 (1999)
12. E. CuChe, P. Marquet and C. Depeursinge, "Aperture apodization using cubic spline interpolation: application in digital holographic microscopy," *Optics Communications* **182**, 59-69, (2000).
13. E. CuChe, P. Marquet and C. Depeursinge, "Spatial filtering for zero-order and twin-image elimination in digital off-axis holography," *Applied Optics* **39**, 4070-4075, (2000).
14. F. Montfort. "Tomography using multiple wavelengths in digital holographic microscopy" (2005).
15. T. Colomb, F. Montfort, J. Kühn, N. Aspert, E. CuChe, A. Marian, F. Charrière, S. Bourquin, P. Marquet and Ch. Depeursinge, "Numerical parametric lens for shifting, magnification and complete aberration compensation in digital holographic microscopy", *J. Opt. Soc. Am. A* **23**, 3177-3190 (2006).